

Intrinsic Birefringence of Amorphous Poly(Bisphenol-A Carbonate)

MAAN-SHII S. WU, *Packaging Systems Division Laboratory, 3M Company, St. Paul, Minnesota 55144*

Synopsis

The birefringence of uniaxially oriented poly(bisphenol-A carbonate) (PC) samples stretched over a wide range of temperatures has been measured accurately with a combination of the compensator and the wedge methods. The Hermans' orientation function of anisotropic PC was calculated from the measured dichroic ratio of the infrared absorption band at 1364 cm^{-1} . Measurements using differential scanning calorimetry, X-ray diffraction, or infrared spectroscopy indicated no stress-induced crystallinity in stretched amorphous PC. At each state having a defined molecular orientation, samples stretched below the glass transition temperature (T_g) always exhibited excess birefringence and slightly higher density. This phenomenon is attributed to bond distortion during stretching, a result of the suppression of large-scale segmental motions of polymer chains below the T_g . The birefringence of samples stretched above the T_g arises exclusively from the orientation effect as a result of greater chain mobility. These measured birefringence values are proportional to Hermans' orientation functions, yielding a linear relationship which allows precise determination of the intrinsic birefringence of amorphous PC as 0.192 ± 0.006 .

INTRODUCTION

During the last decade, poly(bisphenol-A carbonate) (PC) has become an important engineering plastic because of its high impact resistance and dimensional stability at normal service temperatures. PC's relatively high glass transition temperature (T_g) and low tendency to crystallize have made it a subject of much study in the amorphous state, where birefringence is frequently used to represent molecular orientation. In the literature, a number of examples have been presented to correlate molecular anisotropy with mechanical properties of glassy polymers^{1,2}; however, very little has been reported on amorphous PC, possibly due to the lack of a simple, precise way of quantifying its molecular orientation. It is shown by Robertson and Buenker³ that Young's modulus of uniaxially stretched PC film is proportional to the "affine molecular orientation" at low strain. Another study⁴ attempted to measure the segmental orientation of PC with the inclusion of fluorescent probes. Researchers in both studies expressed the need for quantitative determination of the orientation function.

Birefringence, infrared spectroscopy (IR), and sonic modulus techniques have been widely used to determine the orientation function of amorphous polymers. In each case a specific parameter—such as the intrinsic birefringence (Δ^0)—is required. In addition, wide angle X-ray scattering (WAXS) has proved to be an effective measurement of the complete orientation function of amorphous poly(ethylene terephthalate) (PET)⁵ and PC.⁶ In one of his pioneering studies using WAXS,⁶ Biangardi determined

the Δ^0 of amorphous PC as 0.236 ± 0.004 , which happens to be 14% higher than the theoretical value of 0.207^7 calculated from bond polarizabilities. Although he considered these values to be in good agreement with each other, Biangardi's higher experimental value may arise from his attempt to least-square fit a group of mixed birefringence data, obtained from stretching samples below and above the T_g .

In this laboratory an effort was made to correlate the crazing behavior of uniaxially stretched PC with its molecular orientation determined by IR and birefringence methods. Depending on the stretching temperatures—either above or below the T_g —anisotropic film samples having the same degree of orientation based on IR measurements exhibited remarkable differences in interference patterns and the measured birefringence. The differences became more and more pronounced as the degree of stretching increased. Film stretched below the T_g always exhibited higher birefringence. In this study, the importance of this disparate optical response is investigated. The Δ^0 is derived from the birefringence produced solely by chain orientation.

THEORY

Different types of birefringence have been discussed by Stein and Tobolsky,⁸ Saunders,⁹ and Ward.¹⁰ In an oriented state, a group of intrinsically anisotropic elements exhibits so-called orientational birefringence (Δ_o) as a result of preferential alignment of these elements. Since the Δ^0 is the maximum of Δ_o , Δ_o is the only birefringence that ought to be and has been¹¹⁻¹⁴ measured to determine the Δ^0 of polymers. While optical anisotropy caused by chain orientation is a direct result of the intrinsic nature of chain segments constituting the polymer, other factors may contribute to the total measured birefringence as well. The application of external stress to polymers can produce a distortional (deformation) birefringence (Δ_d) from slight changes in intermolecular distances or distortion of bond angles and bond lengths. This kind of birefringence is normally small in magnitude because of large interatomic forces opposing such deformation. In multiphase systems, on the other hand, there exists form birefringence (Δ_f) which is associated with structural or shape anisotropy stemming from refractive index discontinuity.¹⁵ The Δ_f usually amounts to less than 10% of the total birefringence and is often neglected in the case of semicrystalline polymers.

Birefringence has become by far the easiest and most rapid measurement that can be made to characterize polymer orientation. In the absence of Δ_d , the average molecular orientation function (f_{av}) in any two-phase system can be related to the measured birefringence according to the following equations^{16,17}:

$$f_{av} = \beta f_c + (1 - \beta) f_{am} \quad (1)$$

$$\Delta_T = \Delta_c^0 \beta f_c + \Delta_{am}^0 (1 - \beta) f_{am} + \Delta_f \quad (2)$$

where β is the crystallinity, f_c and f_{am} are the Hermans' orientation functions¹⁸ for the crystalline and amorphous phases, respectively, Δ_T is the total measured birefringence, and Δ_c^0 and Δ_{am}^0 are the intrinsic bire-

fringence of the crystalline and amorphous phases, respectively. For a completely amorphous polymer, in which β and Δ_f become zero, eqs. (1) and (2) are reduced to

$$f_{av} = f_{am} \quad (3)$$

$$\Delta_T = \Delta_o = \Delta_{am}^o f_{am} \quad (4)$$

Equation (4) predicts a straight line relationship between Δ_T and f_{am} with a slope equivalent to Δ_{am}^o . However, it should be reemphasized that eqs. (2) and (4) are valid only where chemical bonds of the polymers are not distorted to any appreciable extent. This point becomes vitally important in the study of stretching polymers—such as PC—that have a high T_g .

Of various techniques developed for measuring polymer orientation, IR is unique in that it can be used to measure quantitatively the crystalline and amorphous orientation functions separately. With the theory originated by Fraser^{19,20} and elaborated by Samuels,²¹ Hermans' orientation function (f) of a uniaxially oriented sample relates to the dichroic ratio (D) of the IR absorption band as follows:

$$f = \frac{(D - 1)(D_0 + 2)}{(D + 2)(D_0 - 1)} \quad (5)$$

where D_0 is the dichroic ratio of the absorption band in a perfectly oriented sample. It is equal to $2 \cot^2 \alpha$, where α is the angle between the polymer chain direction and the transition moment of the particular vibrational mode involved. Equation (5) permits determination of the f by measuring D of the IR absorption having a known α . In the IR spectrum of amorphous PC, the band at 1364 cm^{-1} has been assigned with confidence to the methyl in-phase symmetric bending modes $\delta_s^i \text{C}(\text{CH}_3)_2$ of the isopropyl groups.²²⁻²⁴ These vibrational modes have $\alpha = 90^\circ$ because their transition moments lie along the bisector of the $\text{CH}_3\text{—C—CH}_3$ bond angles and are perpendicular to the polymer chain axis (Fig. 1). In this study the f of various stretched film samples is calculated taking advantage of this structural parameter provided by the 1364 cm^{-1} band.

EXPERIMENTAL

Material

Commercial PC, Merlon MPG-700, was kindly supplied by Patricia B. Etta of the Mobay Chemical Co., Pittsburg, PA. The polymer is a clear extrusion-grade resin with a weight average molecular weight of 48,700, as determined by gel permeation chromatography, and a $T_g = 150^\circ\text{C}$, as determined by differential scanning calorimetry (DSC).

Sample Preparation

The resin pellets were dried at 120°C for 3 h prior to extrusion at 325°C into film $0.117 \pm 0.008 \text{ mm}$ thick. This extruded film was cut into several 0.5-in. wide strips, each registered with a mark 2-in. long. Film 0.5×10^{-2}

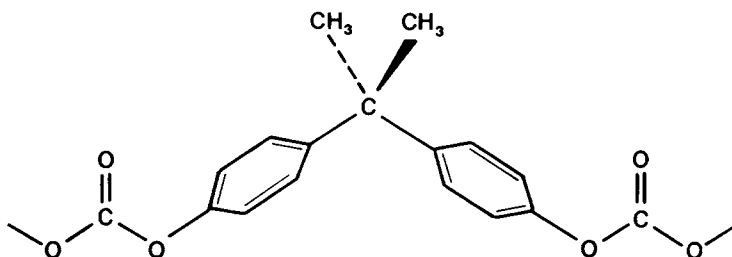


Fig. 1. Fully extended chain conformation of PC.

mm thick was also cast manually at room temperature from a 10% PC solution in methylene chloride onto a glass microscope slide using a #31 Meyer rod. All specimens were then stretched in the length direction using an Instron Tensile Tester (M-S table model) equipped with a heating chamber controlled to within $\pm 0.5^\circ\text{C}$. Each stretching was carried out to a predetermined draw ratio using various combinations of crosshead speeds and stretching temperatures. At completion the film, still being held between the jaws, was immediately cooled to ambient temperature, then removed, and stored for 2–6 weeks before physical properties were measured.

Birefringence

The birefringence of oriented films was measured using a Zeiss polarizing microscope and an Ehringhaus calcite-plate rotary compensator. The procedure followed that described by Samuels.²⁵ However, because of the absence of a black band normally observed at the point of complete compensation, it was necessary in all cases to determine beforehand the highest integer-order of the optical retardation (Γ) using the wedge method.²⁶ The required wedge was cut from a stretched sample and examined under the polarizing microscope using green light ($\lambda = 546 \text{ nm}$). The total number of parallel black fringes observed across this wedge corresponded to the highest integer-order of the optical retardation. This information was then used to help identify the precise point of complete compensation when the stretched sample was reexamined with the compensator.

Infrared Spectroscopic Measurement

IR spectra of stretched films were obtained on a Nicolet-7199 Fourier Transform Infrared (FTIR) Spectrometer. All spectra were recorded at a resolution of 1 cm^{-1} using 200 scans. The spectra of each sample were obtained with the direction of the polarized IR radiation being parallel and perpendicular to the film stretching direction, respectively. The D of the 1364 cm^{-1} band was calculated from an absorbance ratio A_{\parallel}/A_{\perp} , measured according to the baseline procedure of Lunn and Yannas.²⁷

Crystallinity

The density (ρ), DSC, and WAXS methods were applied to determine the stress-induced crystallinity, if any, in stretched films. The ρ was measured to within $\pm 0.0005 \text{ g/cm}^3$ in a density-gradient column containing a solution

at 23°C of isooctane and fluorocarbon FC-77 (registered trademark of 3M Co.). All DSC thermograms were obtained on a Perkin-Elmer DSC-II differential scanning calorimeter. The sample was heated to 200°C, cooled to 20°C, and reheated to 250°C, all at a rate of 20°C/min. X-ray photographs of Laue pattern were taken on a GE XRD-3 diffraction unit with $\text{CuK}\alpha$ 1.5418 Å radiation. The distance between the sample and the photographic film was 5.90 cm and the exposure time was 1.5 h.

RESULTS AND DISCUSSIONS

Anisotropic PC samples were fabricated by stretching the extruded film at two sets of temperature, one set above the T_g (series A) and the other below (series B). Various combinations of draw ratios and stretching rates produced different degrees of film orientation. Given in Tables I and II are the stretching conditions, Δ_T , f , and ρ of each oriented film in series A and B, respectively. Above the T_g , stretching employing a small amount of plastic strain generally yields a marginal molecular orientation. Substantial error could be introduced in determining the f from IR data; thus, only one sample (no. 16) made at a draw ratio smaller than 1.20:1 is presented in Table I. Nevertheless, the lack of precise data in this region can be compensated for by including the theoretical value of the isotropic state in the

TABLE I
Stretching Conditions (Temperature T , Rate R , Draw Ratio DR), Birefringence Δ_T , Orientation Function f , and Density ρ for Series A Samples

Sample no.	T (°C)	R (%/min)	DR	Δ_T	f	ρ (g/cm ³)
1	Extruded film	—	—	0.0001	0.000	1.1978
2	160	100	1.28	0.0122	0.091	1.1986
3	160	100	1.38	0.0158	0.108	1.1977
4	160	100	1.53	0.0199	0.130	1.1975
5	160	100	1.59	0.0212	0.134	1.1977
6	160	100	1.61	0.0243	0.141	1.1979
7	160	100	1.70	0.0241	0.140	1.1979
8	160	100	1.78	0.0275	0.156	1.1990
9	160	100	1.85	0.0270	0.160	1.1981
10	160	100	1.97	0.0303	0.170	1.1977
11	160	100	2.03	0.0338	0.191	1.1986
12	160	100	2.28	0.0358	0.202	1.1988
13	160	100	2.34	0.0361	0.193	1.1990
14	160	100	2.52	0.0388	0.218	1.1990
15	160	100	2.75	0.0424	0.225	1.1979
16	160	250	1.17	0.0076	0.054	1.1970
17	160	250	1.47	0.0177	0.099	1.1978
18	160	250	1.66	0.0210	0.105	1.1980
19	160	50	1.95	0.0231	0.133	1.1983
20	160	250	1.97	0.0241	0.137	1.1978
21	160	50	2.94	0.0278	0.158	1.1985
22	170	1000	2.63	0.0235	0.147	1.1975
23	170	2500	2.88	0.0261	0.148	1.1981
24	170	1250	2.96	0.0285	0.151	1.1975
25	170	5000	3.01	0.0306	0.163	1.1981
26	170	2500	3.15	0.0332	0.179	1.1978

TABLE II
Stretching Conditions (Temperature T , Rate R , Draw Ratio DR), Birefringence $\Delta\tau$,
Orientation Function f , and Density ρ for Series B Samples

Sample no.	T (°C)	R (%/min)	DR	$\Delta\tau$	f	ρ (g/cm ³)
1	23	50	1.61	0.0379	0.157	1.2013
2	23	50	1.75	0.0422	0.149	1.2003
3	23	50	1.84	0.0455	0.164	1.2010
4	23	25	2.03	0.0477	0.196	1.2018
5	23	50	2.03	0.0476	0.168	1.2007
6	23	100	2.03	0.0496	0.207	1.2013
7	23	100	2.05	0.0496	0.212	1.2007
8	23	50	2.09	0.0485	0.186	1.2014
9	23	50	2.20	0.0531	0.199	1.2013
10	23	10	2.31	0.0548	0.220	1.2010
11	65	1000	2.28	0.0569	0.227	1.2010
12	99	1000	2.44	0.0593	0.236	1.2007
13	120	250	2.64	0.0660	0.242	1.2022
14	130	250	2.66	0.0658	0.271	1.2016

calculation. On the other hand, films stretched at room temperature at draw ratios lower than 1.61:1 are not uniform because of the well-known yielding phenomenon of PC; hence, they are excluded in Table II.

Before proceeding to discuss the presented data, it must be pointed out that, in using the compensator to measure birefringence, the black band normally observed at the point of complete compensation is generally absent in the case of stretched PC. Instead, one observed interference bands having other distinct colors depending on the increasing optical retardation of the sample. The color first appears as dark blue ($\Gamma < 1300$ nm), changes to a rust-cyan (1300 nm $< \Gamma < 2500$ nm), to a blue-purple (2500 nm $< \Gamma < 3000$ nm), and finally becomes a bright purple-yellow ($\Gamma \geq 3000$ nm). At $\Gamma < 1300$ nm, the dark blue band observed with a symmetrical Newton-scale interference pattern on both sides can be identified unambiguously as the exact point of complete compensation. However, at higher values of Γ , such a symmetrical interference pattern did not exist around the aforementioned distinct bands. This leads one to speculate whether these nonblack, pseudocompensating bands do in fact coincide with the point of complete compensation. When the successive integer-order retardation of the wedge specimen of each stretched film was offset using the compensator, it was discovered that the genuine compensating band indeed changed its interference color from a true black to a longer-wavelength color as Γ increased with increased specimen thickness. This explains why the traditional black band was missing. To the best of the author's knowledge, this unusual phenomenon of missing black compensating band in anisotropic PC has never been elaborated in the literature. It may be a result of a combination of the following factors: (1) significant dispersion of birefringence in PC, as reported by Cloud²⁸; (2) substantial dispersion of birefringence of the compensator's calcite plate associated with high phase differences at the point of compensation; and (3), most importantly, considerable differences in dispersion of birefringence between PC and the calcites. Because of the missing black band, the wedge method was necessary for complementing the com-

pensator technique to measure values of Γ greater than 1300 nm. In these cases the band which is one order below that exhibiting the most distinct interference colors, as described above, corresponds to the point of complete compensation.

To demonstrate the effectiveness of coordinating the compensator and the wedge methods to measure Γ , two pieces of thinner extruded films (3.8×10^{-2} mm) were stretched at 23°C using a 50%/min rate. The stretched films exhibited Γ values of 1000 and 1138 nm, measured by the unequivocal presence of the dark blue band as discussed previously. The calculated Δ_T values, 0.0346 and 0.0471, for specimens having draw ratio of 1.55 and 2.05 to 1, respectively, are comparable to those obtained from stretching thick samples: e.g., nos. 1 and 4–8 in Table II, a result which indicates the validity of this approach.

In the plot (Fig. 2) of Δ_T vs. f for each stretched film in both series, not all data fit the theoretical single straight line. Instead, Δ_T can be considered linearly proportional to f only within each series. The stretching rates do not significantly affect the linearity of these relationships. The rate of increase of birefringence with respect to the molecular orientation is dependent only on the stretching temperature; e.g., a higher rate when films were stretched below the T_g . This type of dependence is very common for a number of glassy polymers (29–35). Assuming that the increase in Δ_T of series A films stems exclusively from the alignment of polymers in the stretching direction, then the excess birefringence gained by the same degree of molecular orientation in series B may be attributed to the occurrence of either crystallization, or chain distortion, two phenomena which affect the measured Δ_T . Crystal formation in the amorphous matrix contributes in different ways to optical anisotropy and to the onset of Δ_p , while chain distortion introduces Δ_d . In the following discussion, these possibilities and conclusions based on density, DSC, X-ray diffraction and IR results will be examined.

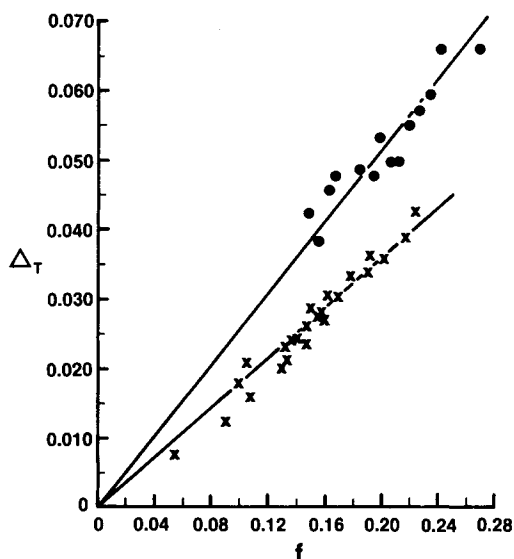


Fig. 2. Plot of total birefringence Δ_T vs. Hermans' orientation function f for all stretched PC samples: (x) series A; (●) series B.

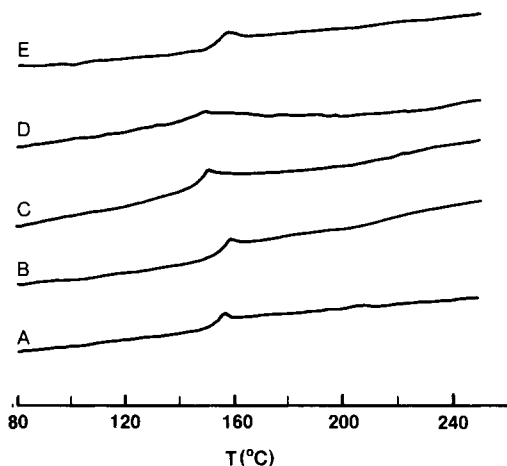


Fig. 3. Representative DSC curves of stretched PC samples: (A) no. 16; (B) no. 17; (C) no. 6; (D) no. 12 in Table I; (E) no. 6 in Table II.

In Table I, the unoriented extruded film (sample no. 1) has a density of 1.1978 g/cm^3 , representing a completely amorphous material.^{36,37} In comparison with this amorphous sample, all oriented films in series A showed very little density deviations which are within the experimental error of the measurement. Therefore, one can conclude that the crystallinity in this series of stretched films is either absent or negligible. DSC measurements provide further support for this conclusion. No endothermic peaks were ever recorded in the region between 210 and 240°C, where the melting point of folded-chain crystalline PC was previously reported.³⁶⁻³⁸ The DSC scans of several representative samples are shown in Figure 3. Without crystallization, preferential orientation of amorphous polymer chains does not change the density of the material.

In contrast to series A, all series B films (Table II) have slightly higher density than the completely amorphous material. If induced-crystallization occurs during stretching, the range of density increase should amount to 2-4% crystallinity according to the following equation³⁹:

$$w^c = \frac{1/\rho - 1/\rho_{\text{am}}}{1/\rho_c - 1/\rho_{\text{am}}} \quad (6)$$

where w^c is the weight fraction crystallinity, ρ is the density of the stretched film, while ρ_{am} (1.198 g/cm^3) and ρ_c (1.315 g/cm^3 ⁴⁰) are the densities of completely amorphous and crystalline PC, respectively. However, the presence of such crystallinity in all series B films was not detected from DSC measurements. A typical DSC thermogram is given at the top (trace E) of Figure 3, again with no melting peak of the crystalline PC. The same conclusion is reached when the Laue X-ray diffraction pattern of sample no. 7 (Fig. 4) in this series is compared with that of the completely amorphous PC (Fig. 5). In both patterns, only one diffuse diffraction at a Bragg's angle $2\theta = 16.97^\circ$ could be identified. This diffraction was reported by Neki and Geil⁴¹ as originating from amorphous PC. The discrete diffraction arcs

observed for the stretched film verify the presence of an oriented phase. Nevertheless, as noted earlier, this anisotropy did not alter the density of the material to any measurable extent.

In order to further confirm the absence of crystallinity in series B, the solution-cast film was stretched 20% using a 2.5%/min rate at 23°C, yielding a birefringence of 0.0333 and an orientation function of 0.118. The carbonyl absorption in the IR spectra remained at 1775 cm^{-1} (Fig. 6), indicating a completely amorphous conformation⁴² for both the cast and stretched films.

It is well known that PC, although crystallizable, does not readily crystallize under normal conditions. Crystallization usually requires specific environments; e.g., exposure to vapors or liquids of low-molecular-weight plasticizers,^{43,44} long annealing in the neighborhood of the T_g ,^{45,46} or inclusion of nucleating agents.^{38,47} These recognized difficulties, combined with the evidence discussed above, lead to the conclusion that stretching of amorphous PC, either above or below its T_g in this study, does not induce crystallization.

Without induced crystallinity, the observed increase in density and gain in birefringence for series B films could result from changes taking place at the molecular level. When subjected to uniaxial drawing at considerable speeds, PC chains orient and align themselves parallel to the stretch direction. However, because of the suppression of major chain-segmental motions at temperatures below the T_g , these chains also must undergo other deformation, especially before yielding begins, in order to relieve part of the applied stress. Very likely, the low-temperature transition mechanisms reported for PC⁴⁸⁻⁵¹ are not dynamic enough to allow for the total release of stress; instead, bond angles of the polymer backbone are expanded slightly as a result of restricted molecular rotations about the single bonds. This bond distortion permits polymer chains in the amorphous phase to be closer with each other, thus reducing the free volume and producing samples of slightly higher bulk density than in the undistorted state. Similarly, the same kind of bond distortion also reorients the symmetry axes of the most polarizable phenyl rings, causing them to align in a direction closer to the polymer chain axis (Fig. 1). This conformation results in an extra amount

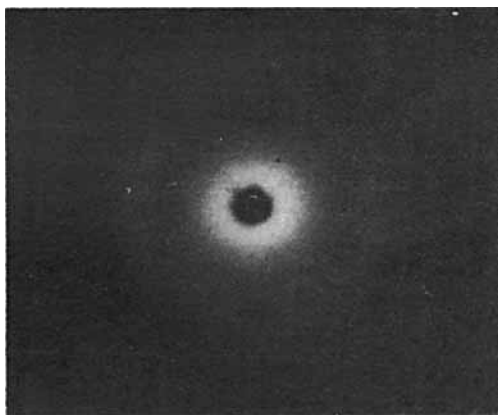


Fig. 4. Back-reflection Laue X-ray diffraction pattern of stretched PC sample no. 7 in Table II.

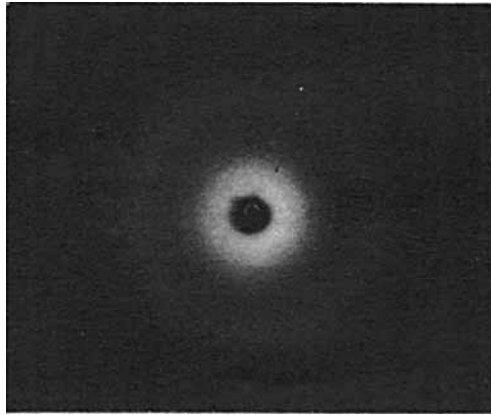


Fig. 5. Back-reflection Laue X-ray diffraction pattern of extruded PC sample no. 1 in Table I.

of birefringence beyond that due to the undistorted state. It has been suggested that bond distortion caused by elastic deformation in the glassy state accounts for the unusual photoelasticity observed in polystyrene,³⁰ poly(vinyl chloride),³² and poly(methyl methacrylate).⁵² For PC the extremely high T_g and lack of large side groups suggest that slight expansion in backbone bond angles is a possible way of intramolecular deformation which responds to the elastic tensile strain. It is, therefore, concluded that the Δ_T measured for all series B films cannot be used to determine Δ^0 because of contributions arising from both chain orientation and bond distortion.

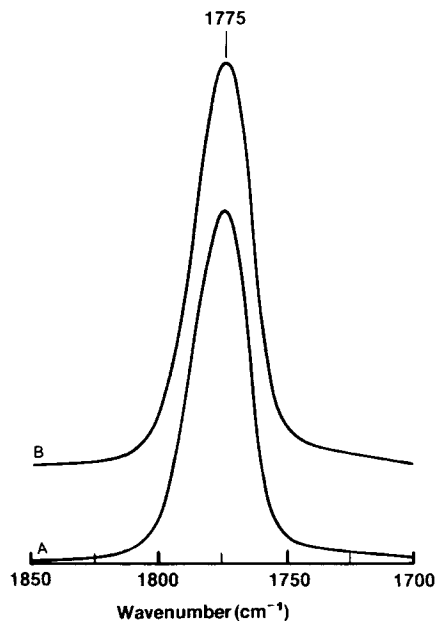


Fig. 6. FTIR spectra in the Range of $1700\text{--}1850\text{ cm}^{-1}$ of (A) unstretched and (B) stretched solution-cast PC film.

The interpretation of the preceding paragraph is based on molecular mobilities. It is consistent with results observed for series A films. The chance for bond distortion during stretching above the T_g is negligible or nonexistent because of the significant onset of large-scale segmental mobility in each polymer chain. Consequently, any noticeable change in density due to the effect of bond distortion is not detected, an observation verified by the data in Table I. In the absence of bond distortion and induced crystallinity, each Δ_T for series A films represents the value expected from the orientation effect alone. Applying eq. (4), a least-square analysis of these data, including that of the unoriented sample, yields the following linear relationship:

$$\Delta_T = \Delta_o = 0.192 \times f - 0.002 \quad (7)$$

with a coefficient of determination $R^2 = 0.97$. The Δ_{am}^0 of PC is then taken as the slope of eq. (7), 0.192 ± 0.006 allowing for experimental error. This value agrees better with the maximum theoretical value of 0.207⁷ than the $\Delta_{am}^0 = 0.236 \pm 0.004$ reported by Biangardi.⁶ Biangardi reported only six birefringence readings obtained from stretching the PC samples to a constant draw ratio between 110 and 175°C. He did not specify the draw temperature for each sample, and the present study indicates that the three highest birefringence values would have reflected a certain amount of bond distortion. Possibly, Biangardi's higher Δ_{am}^0 was a consequence of his having used least-square fit involving these three readings.

Both the orientation and distortion of polymer chains contribute to the measured Δ_T of films in series B. It is worth investigating how significant the error would be if data obtained from below T_g stretching were included in the calculation of Δ^0 . As shown in Figure 2, the Δ_T - f relationship for series B films is also fairly linear, implying that the degree of bond distortion, as measured by the excessive optical anisotropy, is also proportional to the overall f of the sample. A least-square analysis of these data results in:

$$\Delta_T = \Delta_o + \Delta_d = 0.244 \times f + 0.002 \quad (8)$$

Combining this equation with eq. (7), one obtains

$$\Delta_d = \Delta_d^0 \times f = 0.05 \times f \quad (9)$$

The symbol Δ_d^0 stands for the specific distortional birefringence relative to the f in stretched amorphous PC. The value of 0.05 for Δ_d^0 is approximately 26% of the Δ_{am}^0 , indicating the possibility of substantial error if any datum obtained from the below- T_g stretching were used to determine Δ^0 .

The value of Δ_{am}^0 for PC, 0.192 as determined in this work, is comparable to the values reported for PET, 0.190¹¹ and 0.204.¹² Examination of the fully extended chain conformations of both polymers suggests some kind of consistency. The major contribution to Δ^0 comes from easily polarizable π electrons in the phenyl rings. At first it would seem that PC has a higher Δ^0 because of the greater number of phenyl rings in each structural repeat unit. However, the angle between the chain direction of PC and the sym-

metry axes of phenyl rings, which exhibit the largest polarizability,⁵³ is larger than that of PET; thus, the polarizability contribution of phenyl π electrons to the Δ^0 in the direction along the polymer chain is reduced. This intramolecular angular effect may explain similar Δ_{am}^0 values in both PC and PET.

CONCLUSION

The intrinsic birefringence of amorphous poly(bisphenol-A carbonate) has been determined from data based on a large number of samples. Considerable caution is required to use the compensator for measuring large-value birefringence of anisotropic PC. The absence of the black band normally observed at the point of complete compensation is attributed to the dispersion of birefringence in both the PC and compensator's tilting calcite plate. Stress-induced crystallization, which could complicate the determination of intrinsic birefringence, does not occur in uniaxially stretched amorphous PC; any complication that could arise from chain distortion can be avoided by drawing the samples at temperatures above the T_g . Only in the absence of crystallization and chain distortion can the total birefringence measured from these uniaxially stretched samples be attributed exclusively to the chain orientation effect and be used to determine precisely the intrinsic birefringence.

It is worth reemphasizing that stretching PC below its T_g causes the bond angles of the polymer backbone to distort, resulting in a detectable contribution to the total measured birefringence. Since this distortion may also influence material properties considered to be orientation-dependent, studies of the exact relationship between the orientation function and the distortional birefringence, when PC is deformed below its T_g , may serve to characterize slight variations in these properties.

The author is grateful to P. B. Etta of the Mobay Chemical Co. for providing the poly(bisphenol-A carbonate) resin used in this study.

References

1. T. T. Jones, *Pure Appl. Chem.*, **45**, 39 (1976).
2. H. Wright, C. S. N. Faraday, E. F. T. White, and L. R. G. Treloar, *J. Phys. D.*, **4**, 2002 (1971).
3. R. E. Robertson and R. J. Buenker, *J. Polym. Sci., A*, **2**, 4889 (1964).
4. H. Springer, R. Neuert, F. D. Müller, and G. Hinrichsen, *Colloid Polym. Sci.*, **261**, 800 (1983).
5. H. J. Biangardi, *J. Polym. Sci., Polym. Phys. Ed.*, **18**, 903 (1980).
6. H. J. Biangardi, *Makromol. Chem.*, **183**, 1785 (1982).
7. B. von Falkai, G. Spilgies, and H. J. Biangardi, *Angew. Makromol. Chem.*, **108**, 41 (1982).
8. R. S. Stein and A. V. Tobolsky, *Text. Res. J.*, **18**, 201 (1948).
9. D. W. Saunders, in *Physics of Plastics*, P. D. Ritchie, Ed., Van Nostrand, Princeton, NJ, 1965, pp. 399-402.
10. I. M. Ward, *Structure and Properties of Oriented Polymers*, Wiley, New York, 1975, pp. 60-64.
11. S. K. Garg, *J. Appl. Polym. Sci.*, **27**, 2857 (1982).
12. V. B. Gupta and S. Kumar, *J. Polym. Sci., Polym. Phys. Ed.*, **17**, 1307 (1979).
13. J. H. Dumbleton, *J. Polym. Sci., A-2*, **6**, 795 (1968).
14. E. Balcerzyk, W. Kozłowski, E. Wesółowska, and W. Lewaszkiewicz, *J. Appl. Polym. Sci.*, **26**, 2573 (1981).

15. O. Wiener, *Abhandl. Kgl. Sächs. Ges. Wiss. Math. Physik. Kl.*, **32**, 509 (1912).
16. R. S. Stein, *J. Polym. Sci.*, **34**, 709 (1959).
17. R. J. Samuels, *Structured Polymer Properties*, Wiley, New York, 1974, p. 20.
18. J. J. Hermans, P. H. Hermans, D. Vermaas, and A. Weidinger, *Rec. Trav. Chim.*, **65**, 427 (1946).
19. R. D. B. Fraser, *J. Chem. Phys.*, **21**, 1511 (1953).
20. R. D. B. Fraser, in *Analytical Methods of Protein Chemistry*, P. Alexander and R. J. Block, Eds., Pergamon, New York, 1960, Vol. 2, Chap. 9.
21. R. J. Samuels, *J. Polym. Sci.*, **A3**, 1741 (1965).
22. W. Brügel, *An Introduction to Infrared Spectroscopy*, Wiley, New York, 1962.
23. L. J. Bellamy, *The Infra-Red Spectra of Complex Molecules*, Wiley, New York, 1958, pp. 13, 24.
24. S. Krimm, personal communication, 1971; cited by A. C. Lunn and I. V. Yannas, *J. Polym. Sci., Polym. Phys. Ed.*, **10**, 2189 (1972).
25. R. J. Samuels, *Structured Polymer Properties*, Wiley, New York, 1974, pp. 55–57.
26. E. F. Gurnee, *J. Appl. Phys.*, **25**, 1232 (1954).
27. A. C. Lunn and I. V. Yannas, *J. Polym. Sci., Polym. Phys. Ed.*, **10**, 2189 (1972).
28. G. Cloud, *J. Opt. Soc. Am.*, **60**, 1042 (1970).
29. H. Kolsky, *Nature*, **166**, 235 (1950).
30. J. F. Rudd and E. F. Gurnee, *J. Appl. Phys.*, **28**, 1096 (1957).
31. J. F. Rudd and R. D. Andrews, *J. Appl. Phys.*, **29**, 1421 (1958).
32. A. Utsuo and R. S. Stein, *J. Polym. Sci., A-2*, **5**, 583 (1967).
33. S. Hibi, M. Maeda, H. Kubota, and T. Miura, *Polymer*, **18**, 137 (1977).
34. H. A. Robinson, R. Ruggy, and E. Slantz, *J. Appl. Phys.*, **15**, 343 (1944).
35. M. Pick, R. Lovell, and A. H. Windle, *Polymer*, **21**, 1017 (1980).
36. J. L. Kalwak, D. J. van Dijk, and J. H. Gisolf, *Colloid Polym. Sci.*, **255**, 428 (1977).
37. G. E. Wissler and B. Crist, Jr., *J. Polym. Sci., Polym. Phys. Ed.*, **18**, 1257 (1980).
38. F. Gallez, R. Legras, and J. P. Mercier, *Polym. Eng. Sci.*, **16**, 276 (1976).
39. B. Wunderlich, *Macromolecular Physics*, Academic, New York, 1973, Vol. 1, p. 385.
40. R. Bonart, *Makromol. Chem.*, **92**, 149 (1966).
41. K. Neki and P. H. Geil, in *The Solid State of Polymers*, P. H. Geil, E. Baer, and Y. Wada, Eds., Marcel Dekker, New York, 1974, pp. 295–341.
42. M. M. Coleman, D. F. Varnell, and J. P. Runt, in *Contemporary Topics in Polymer Science*, W. J. Bailey and T. Tsuruta, Eds., Plenum, New York, 1984, Vol. 4, pp. 807–828.
43. J. P. Mercier, G. Groeninckx, and M. Lesne, *J. Polym. Sci., Part C*, **16**, 2059 (1967).
44. R. Legras and J. P. Mercier, *J. Polym. Sci., Polym. Phys. Ed.*, **15**, 1283 (1977).
45. A. Siegmann and P. H. Geil, *J. Macromol. Sci. Phys.*, **B4**, 239 (1970).
46. A. Siegmann and P. H. Geil, *J. Macromol. Sci. Phys.*, **B4**, 273 (1970).
47. R. Legras, J. P. Mercier, and E. Nield, *Nature*, **304**, 432 (1983).
48. K. Varadarajan and R. F. Boyer, *J. Polym. Sci., Polym. Phys. Ed.*, **20**, 141 (1982).
49. K. H. Illers and H. Breuer, *Kolloid Z.*, **176**, 110 (1961).
50. T. Hara and S. Okamoto, *J. Appl. Phys. (Jpn.)*, **3**, 499 (1964).
51. J. H. Golden, B. L. Hammant, and E. A. Hazell, *J. Appl. Polym. Sci.*, **11**, 1571 (1967).
52. M. Pick and R. Lovell, *Polymer*, **20**, 1448 (1979).
53. B. Erman, D. Wu, P. A. Irvine, D. C. Marvin, and P. J. Flory, *Macromolecules*, **15**, 670 (1982).

Received June 19, 1985

Accepted January 21, 1986